Proc. of the 9th Intl. Conf. of Asian Society for Precision Engg. and Nanotechnology (ASPEN 2022)
15–18 November 2022, Singapore. Edited by Nai Mui Ling Sharon and A. Senthil Kumar
doi://10.3850/978-981-18-6021-8_OR-01-0269

Laser Powder Bed Fusion of Grain Refined 316L Stainless Steel through Ti in-situ Alloying

Wengang Zhai[1], Wei Zhou[1,2,#], and Sharon Mui Ling Nai[3,#]

1 School of Mechanical and Aerospace Engineering, Nanyang Technological University, 50 Nanyang Avenue, 639798, Singapore
2 Singapore Centre for 3D Printing, school of Mechanical and Aerospace Engineering, Nanyang Technological University, 50 Nanyang Avenue, 639798, Singapore
3 Singapore Institute of Manufacturing Technology, 73 Nanyang Drive, 637662, Singapore
Corresponding Author / Email: wzhou@cantab.net, mwzhou@ntu.edu.sg (W. Zhou), TEL: +65-67904700, FAX: +65-67924062
Corresponding Author / Email: mlnai@simtech.a-star.edu.sg (S.M.L. Nai), TEL: +65-67938976

KEYWORDS: Additive manufacturing, Laser powder bed fusion, Grain refinement, 316L stainless steel, In-situ alloying, Alloy design

Laser powder bed fusion (LPBF) is a subset of additive manufacturing process, which has the advantage in the fabrication of geometry-complex components. It features a high thermal gradient because of the intrinsic ultrafast cooling rate (~10^7 K/s). The high thermal gradient leads to a higher critical nucleation undercooling and the fast cooling rate limits the formation of solutes. Consequently, strong epitaxial grain growth tendency is frequently observed in LPBF-processed alloys. This presentation demonstrates that in-situ alloying with Ti addition can significantly promote grain refinement (from 16.7 to 0.8 μm) without bringing undesirable intermetallic phases in LPBF-processed 316L. The Ti-rich solutes at the solid/liquid interface activated heterogeneous nucleation, thus achieving grain refinement. This method could also be used for the grain refinement of other alloys, such as Al alloys and Ti alloys, in order to tailor their microstructures and mechanical properties to suit specific engineering applications.

NOMENCLATURE

LPBF = laser powder bed fusion
AM = additive manufacturing
SEM = scanning electron microscope
XRD = x-ray diffraction
EBSD = electron backscattered diffraction
LAGB = low angle grain boundary
UTS = ultimate tensile strength
σ_y = yield strength

1. Introduction

Additive manufacturing (AM) is a transformative approach to industrial production due to its layer-by-layer building strategy and thus enable to fabricate geometry-complex components. LPBF is an AM process utilizing a laser as heat source to melt powders. It is one of the most popular metal AM processes because of its high three-dimensional accuracy.

316L stainless steel has a wide range of engineering applications due to its good corrosion resistance, oxidation resistance, formability and weldability [1]. According to ASTM A240, 316L has a low yield strength at 170 MPa. LPBF-processed 316L features elongated grains owing to the high thermal gradient and ultrafast cooling rate resulting in a strong epitaxial grain growth tendency [2, 3]. Compared to conventional processes, LPBF enable to fabricate 316L with a higher yield strength up to 600 MPa [1-6]. However, the elongated grain morphology with a high length-to-width ratio along the building direction of LPBF-processed 316L usually presents an anisotropic mechanical property [7, 8]. A potential way approach to reduce the anisotropic phenomenon is grain refinement.

Grain refinement for LPBF-processed 316L has been successfully achieved through adding foreign particles, such as TiC particles [3, 9, 10]. Most of the alloys are designed for conventional processes, such as casting and forging. However, AM processes have much faster cooling rate. The alloy composition is needed to be modified to avoid the formation of cracks or other defects. Therefore, in-situ alloying has been widely studied for AM processes. In-situ alloying can also be used for the grain refinement. Notable cases of success include modified Aluminum alloys with the addition of Zr/Sc [11].

According to the interdependence theory [12], the grain size in the solidified alloys is determined by the constitutional supercooling, ΔT_{cs}, ahead of the S/L interface. In order to obtain fine and equiaxed grains, a large ΔT_{cs} is preferred because it promotes the presence of adequate solute at the S/L interface. We previously studied the effect of Ti addition to 316L using LPBF process [1]. Here we further analyzed the Ti-induced grain refinement for 316L. Adding Ti to 316L could promotes the formation of solutes at the S/L interface and thus grain refinement could be obtained due to the Fe-Ti eutectic reaction. In this work, low addition of Ti solute was used for grain refinement to avoid the formation of undesirable phase. The microstructures and mechanical properties evolution are investigated.

2. Materials and methods

2.1 Materials

Commercial gas atomized spherical 316L powder (mean size: 42 µm) and pure Ti powder (mean size: 32 µm) were used as feedstock. Scanning electron microscope (SEM) images in Fig. 1a and b show the morphologies of 316L and Ti powders. 0.3, 1.0, 1.5, and 3.0 wt% Ti powder were added to 316L powder and mixed directly at a speed of 20 rpm for 3 hrs. The Ti-modified 316L alloys are labeled as 316L-0.3Ti, 316L-1.0Ti, 316L-1.5Ti and 316L-3.0Ti according to their respective Ti additions.

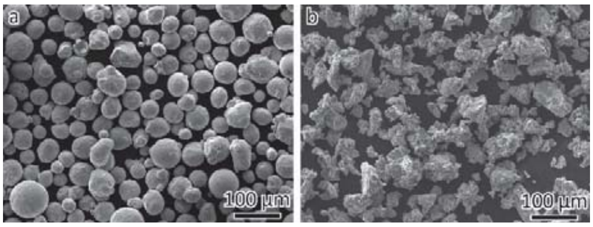

Fig. 1 SEM images showing the morphologies of (a) 316L powder, and (b) pure Ti powder.

2.2 LPBF process

LPBF was performed using a commercial machine (ProX DMP 300, 3D Systems, US). The machine was equipped with a 500 W continuous wave fiber laser (wavelength: 1070 nm). The spot size of the laser beam at the focal point is 75 µm. Ar gas was purged to the printing chamber as a shielding gas. The laser scanning direction was rotated 90° between two adjacent layers. The parameters for 316L are as follows: laser power, 182 W; laser scanning speed, 1000 mm/s; layer thickness, 30 µm; and hatch spacing, 55 µm. Parameter optimization was conducted for Ti-modified 316L. For parameter optimization, laser powers ranging from 150 to 250 W were selected. The scanning speed of 800 mm/s, layer thickness of 30 µm and hatch spacing of 70 µm were kept constant. The tensile samples of Ti-modified 316L were fabricated at a laser power of 225 W.

2.3 Microstructure characterization

The microstructures were studied using Optical Microscope, SEM, X-Ray diffraction (XRD) and Electron Backscattered Diffraction (EBSD). A step size of 0.01° and scanning speed of 0.4°/min were used for XRD measurements. The EBSD step size was 1.5 µm for 316L and 316L-0.3Ti. and 0.6 µm for 316L-1.0Ti.

2.4 Mechanical properties

Microhardness was measured under a 300 g load with a dwell time of 15 s. For each sample, 21 indentations were carried out. For each type of the material, 3 tensile samples were tested at room temperature at a strain rate of 10^{-3} s^{-1} using Instron 5982 universal tensile testing machine. A non-contact Instron AVE 2 extensometer was used to measure the tensile strain. The tensile samples have a size of 14 mm × 4 mm × 2 mm which was prepared using wire cutting.

3. Results

3.1 Parameters optimization of LPBF-processed 316L-Ti

At low laser powers of 150 and 175 W, lack of fusion was observed with the additions of Ti at 0.3, 1.0, and 1.5 wt%. No obvious defects were observed in samples built with the laser powers of 200, 225 and 225 W. After etching, dark areas in the shape of swirls were observed in the samples built with low laser power, as shown in Fig. 5. With the increase of laser power, the fraction of dark areas was decreased. The dark areas represent segregations of Ti.

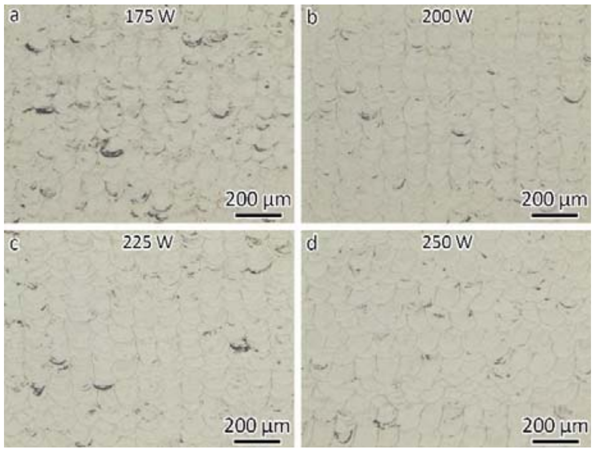

Fig. 2 Optical micrographs showing the microstructures of 316L-1.0Ti fabricated using different laser powers after etching.

3.2 Microstructures evolution

316L is a fully austenitic stainless steel. Adding Ti to 316L promotes the formation of ferrite phase, as shown in the XRD results (Fig. 3). In the sample of 316L-3.0Ti, the ferrite phase peaks are relatively intense when compared with the austenite phase peaks. It is known that Ti is a ferritic phase formation element in stainless steels. Notably, no undesirable phase was detected.

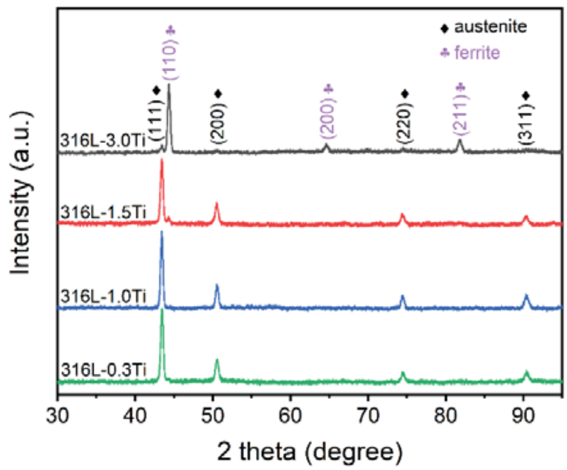

Fig. 3 XRD patterns of Ti-modified 316L.

LPBF-processed 316Lusually has elongated grains due to the intrinsic high cooling rate and thermal gradient. The grain morphology was studied using EBSD (Fig 4). 316L-0.3Ti shows a similar grain morphology to 316L, as shown in Fig. 4a. Adding 1.0 and 1.5 wt% Ti to 316L significantly refined the grains, as shown in Fig. 4b. The grain size of 316L and Ti-modified 316L is shown in Fig. 5. The grain size of 316L, 316L-0.3Ti, 316L-1.5Ti is measured using EBSD according to the high angle grain boundaries (>15°). The grain size of 316L-3.0Ti is measured using intersection method from its BSE image.

It is difficult to fabricate 316L with fine and equiaxed grains using LPBF due to the intrinsic high thermal gradient and fast cooling rate. Under this condition, solutes are difficult to form at the S/L interface. Due to the eutectic reaction of Fe-Ti, adding Ti to 316L promotes the formation of solutes at the S/L interface and thus grain refinement is obtained.

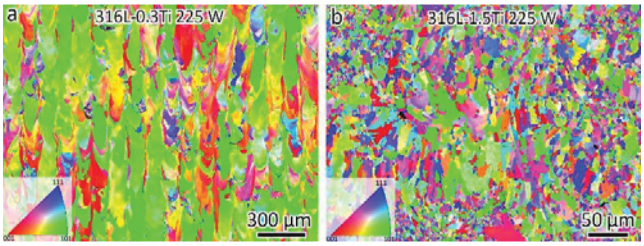

Fig. 4 EBSD results of LPBF-processed 316L-0.3Ti and 316L-1.5Ti showing the grain refinement.

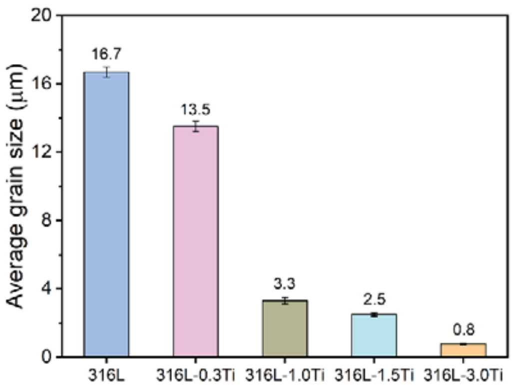

Fig. 5 Average grain size of LPBF-processed 316L and Ti-modified 316L.

The grain boundaries misorientation data can be extracted from EBSD results. LPBF-processed 316L showed a high fraction of low angel grain boundaries (LAGBs, <15°), as shown in Fig. 6a. Adding Ti to 316L impeded the formation of LAGBs, as shown in Fig. 6b, c, and d. A relatively high frequency of 60° misorientation was observed in LPBF-processed 316L-1.0Ti and 316L-1.5Ti, indicating the presence of a large fraction of twin boundaries. The twin boundaries in 316L-0.3Ti, 316L-1.0Ti and 316L-1.5Ti were observed using SEM backscatter electron (BSE) mode without etching the samples, as shown in Fig. 7. During LPBF process, the printed materials experience remelting and thus in-situ heat treatment happens. The annealing twin boundaries in Ti-modified 316L are generated due to the in-situ annealing.

The LPBF-processed 316L-3.0Ti alloy is brittle. Macro cracks were observed during parameter optimization in all 316L-3.0Ti samples. The cracks are intergranular, as shown in Fig. 7d.

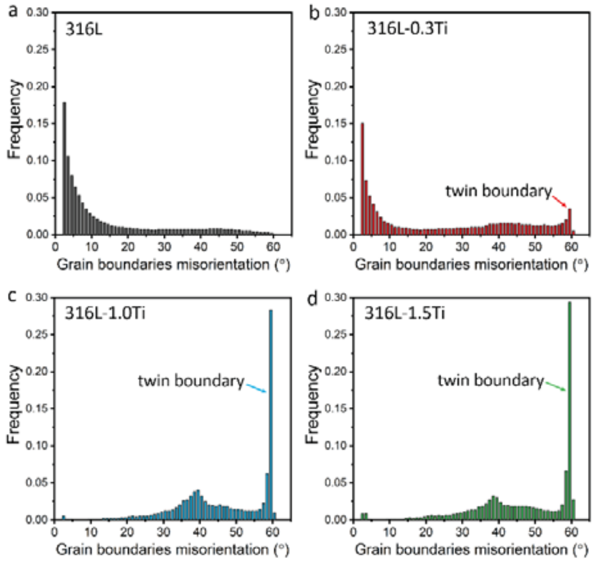

Fig. 6 Grain boundaries misorientation extracted from EBSD results showing the evolution of twin boundary.

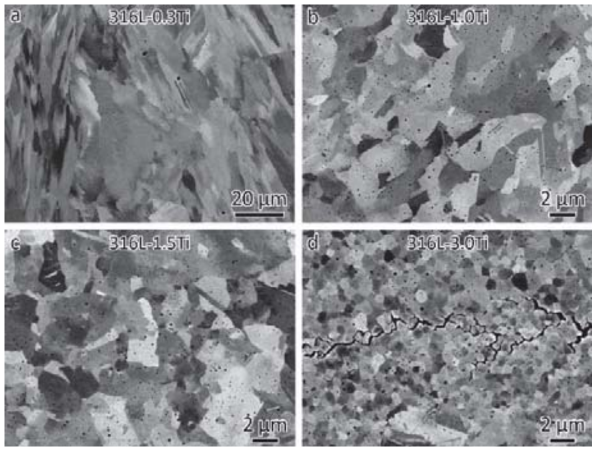

Fig. 7 SEM BSE images showing the presence of twin boundaries and intergranular cracks in Ti-modified 316L.

3.3 Mechanical properties

The microhardness is shown in Fig. 8a. The microhardness of LPBF-processed 316L was 239.6 ± 6.6 HV. The microhardness of 316L is increased with the increase of Ti addition. The microhardness of 316L-3.0Ti was increased significantly, measured at 523.2 ± 42.4 HV. Notably, the standard deviation (error bar) of the microhardness was also increased with increased Ti addition. This is related to the segregation of Ti in the dark area (Fig. 2).

Fig. 8b shows the engineering stress-strain curves. Tensile test on 316L-3.0Ti was omitted since the presence of macro cracks. With the addition Ti, the ultimate tensile strength (UTS) was increased, from 704 MPa for 316L to 817 MPa for 316L-1.5Ti. The yield strength (σ_y) was increased from 581 MPa for 316L to 634 MPa for 316L-1.5Ti. The yield strength of 316L-0.3Ti and 316L-1.0Ti is the same. With

1.5 wt% Ti addition, the total elongation drops from 55 to 29%. The results of the tensile tests are summarized in Table 1.

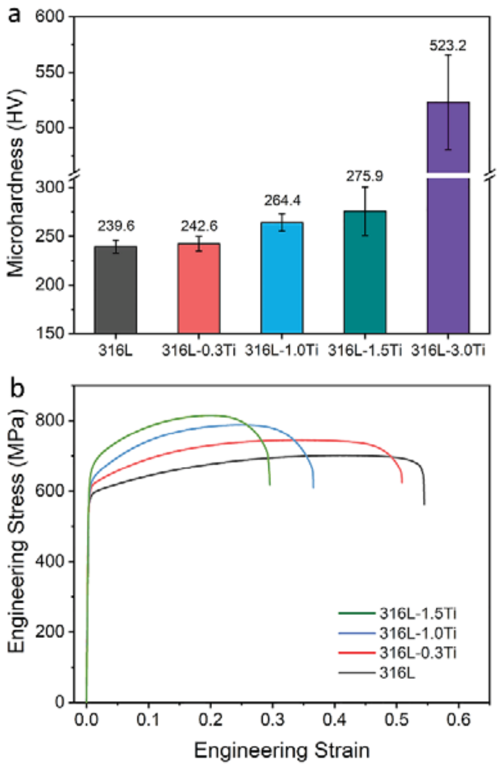

Fig. 8 (a) Microhardness and (b) tensile curves of 316L and Ti-modified 316L.

Table 1 Tensile results of 316L with different Ti addition.

Material	σ_y (MPa)	UTS (MPa)	Elongation (%)
316L	581 ± 7	704 ± 3	55 ± 2
316L-0.3Ti	597 ± 9	745 ± 0.5	51 ± 1
316L-1.0Ti	597 ± 1	785 ± 3	37 ± 0.6
316L-1.5Ti	634 ± 4	817 ± 2	29 ± 0.6

4. Conclusions

(1). In-situ alloying of Ti addition can significantly promote grain refinement (from 16.7 to 0.8 μm) without introducing undesirable intermetallic phases in LPBF-processed 316L;

(2). Addition of 1.0 and 1.5 wt% Ti to 316L promotes the formation of twin boundary. High amount of Ti addition at 3 wt% to 316L results in the formation of macro cracks;

(3). The addition of Ti enhanced the UTS from 704 MPa for 316L to 817 MPa for 316L-1.5Ti. The yield strength is increased from 581 MPa for 316L to 634 MPa for 316L-1.5Ti. The ductility is decreased with the addition of Ti.

ACKNOWLEDGEMENT

The authors acknowledge the support from the Singapore Institute of Manufacturing Technology for access to the Industrial Additive Manufacturing Facility and the support from Nanyang Technological University for access to the materials characterization facilities.

REFERENCES

1. Zhai W., Zhou W., Nai S.M.L., "Grain refinement of 316L stainless steel through in-situ alloying with Ti in additive manufacturing," Mater. Sci. Eng. A. Vol. 840, pp. 142912, 2022.
2. Zhai W., Zhou W., Zhu Z., Nai S.M.L., "Selective Laser Melting of 304L and 316L Stainless Steels: A Comparative Study of Microstructures and Mechanical Properties," Steel Res. Int. Vol. 93, No. 7, pp. 2100664, 2022.
3. Zhai W., Zhou W., Zhu Z., Nai S.M.L., Wei J., "Selective laser melting of dispersed TiC particles strengthened 316L stainless steel," Compos. B. Eng. Vol. 199, pp. 108291, 2020.
4. Wang Y.M., Voisin T., McKeown J.T., Ye J., Calta N.P., Li Z., Zeng Z., Zhang Y., Chen W., Roehling T.T., Ott R.T., Santala M.K., Depond P.J., Matthews M.J., Hamza A.V., Zhu T., "Additively manufactured hierarchical stainless steels with high strength and ductility," Nat. Mater. Vol. 17, No. 1, pp. 63-71, 2018.
5. Liu L., Ding Q., Zhong Y., Zou J., Wu J., Chiu Y.-L., Li J., Zhang Z., Yu Q., Shen Z., "Dislocation network in additive manufactured steel breaks strength-ductility trade-off," Mater. Today. Vol. 21, No. 4, pp. 354-361, 2018.
6. Wei F., Cheng B., Kumar P., Wang P., Lee J.J., Seng H.L., Cheong K.H., Lau K.B., Tan C.C., "A comparative study of additive manufactured and wrought SS316L: Pre-existing dislocations and grain boundary characteristics," Mater. Sci. Eng. A. Vol. 833, pp. 142546, 2022.
7. Shrestha R., Simsiriwong J., Shamsaei N., "Fatigue behavior of additive manufactured 316L stainless steel parts: Effects of layer orientation and surface roughness," Addit. Manuf. Vol. 28 pp. 23-38, 2019.
8. Jeon J.M., Park J.M., Yu J.-H., Kim J.G., Seong Y., Park S.H., Kim H.S., "Effects of microstructure and internal defects on mechanical anisotropy and asymmetry of selective laser-melted 316L austenitic stainless steel," Mater. Sci. Eng. A. Vol. 763, pp. 138152, 2019.
9. Zhai W., Zhou W., Nai S.M.L., "In-situ formation of TiC nanoparticles in selective laser melting of 316L with addition of micronsized TiC particles," Mater. Sci. Eng. A. Vol. 829, pp. 142179, 2022.
10. Zhai W., Zhou W., Nai S.M.L., "Grain refinement and strengthening of 316L stainless steel through addition of TiC nanoparticles and selective laser melting," Mater. Sci. Eng. A. Vol. 832, pp. 142460, 2022.
11. Zhu Z., Ng F.L., Seet H.L., Lu W., Liebscher C.H., Rao Z., Raabe D., Nai S.M.L., "Superior mechanical properties of a selective-laser-melted AlZnMgCuScZr alloy enabled by a tunable hierarchical microstructure and dual-nanoprecipitation," Mater. Today. Vol. 52, pp. 90-101, 2022.
12. StJohn D.H., Qian M., Easton M.A., Cao P., "The Interdependence Theory: The relationship between grain formation and nucleant selection," Acta Mater. Vol. 59, No. 12, pp. 4907-4921, 2011.